Radboud Repository

Radboud University Nijmegen

PDF hosted at the Radboud Repository of the Radboud University Nijmegen

The following full text is a publisher's version.

For additional information about this publication click this link.
http://hdl.handle.net/2066/112831

Please be advised that this information was generated on 2018-07-08 and may be subject to change.

Semicond. Sci. Technol. 5 (1990) 861–866. Printed in the UK

Observation of high mobility and cyclotron resonance in 20 Å silicon δ-doped GaAs grown by MBE at 480 °C

P M Koenraad†, F A P Blom†, C J G M Langerak‡, M R Leys†, J A A J Perenboom‡, J Singleton‡, S J R M Spermon‡, W C van der Vleuten†, A P J Voncken† and J H Wolter†

†Physics Department, Eindhoven University of Technology, PO 513, 5600 MB, Eindhoven, The Netherlands

‡High Field Magnet Laboratory and Research Institute for Materials, University of Nijmegen, Toernooiveld, 6525 ED, Nijmegen, The Netherlands

Received 18 July 1989, accepted for publication 19 April 1990

Abstract. We report on temperature-dependent Hall effect measurements on Si δ-doped GaAs samples grown by MBE at 480 °C, 530 °C and 620 °C. In the best sample grown at 480 °C the mobility is 6760 $cm^2 V^{-1} s^{-1}$ at 4.2 K. To our knowledge this is the highest mobility ever reported in a δ-doped structure. From subband population measurements the spreading of the donors in the samples grown at low temperature is determined to be 20 Å. On these high-mobility samples we were able to perform the first reported cyclotron resonance measurements. The electron effective mass is found to be considerably higher than that at the Γ-conduction band minimum in GaAs.

1. Introduction

Recently there has been a lot of interest in the physics of sharply confined doping layers (δ-doping). Until now δ-doping has been used successfully for Si layers in GaAs and $Al_xGa_{1-x}As$ [1, 2], Sb layers in Si [3] and S layers in InP [4]. Both molecular beam epitaxy (MBE) and metal organic chemical vapour deposition (MOCVD) have been used to grow such δ-doped layers. The two-dimensional nature of the electrons confined in the potential well, induced by the δ-doped donor layer, was first shown from Shunikov–de Haas (SdH) measurements by Zrenner *et al* [1]. It has been shown from secondary ion mass spectrometry (SIMS) [5] and subband population measurements [2, 6] that the spreading of the donors is strongly reduced when the growth temperature is lowered. Recently, Gillman *et al* [7] presented Hall effect measurements of the electron density and mobility in Si δ-doped GaAs samples grown at 590 °C. They reported a maximum Hall mobility of 2000 $cm^2 V^{-1}s^{-1}$ at 4.2 K.

By growing at low temperature, 480 °C, we are able to enhance the mobility at 4.2 K to 6760 $cm^2 V^{-1}s^{-1}$. In this paper we present measurements on the Hall effect and subband population carried out on Si δ-doped GaAs samples grown at 480 °C, 530 °C and 620 °C. We also report cyclotron resonance (CR) measurements on δ-doped samples for the first time.

2. Experiment

The δ-doped samples were grown in our computer-controlled Varian modular MBE system. The semi-insulating GaAs [100] substrates were carefully cleaned and etched before they were introduced into the MBE system. The substrates were annealed at 630 °C in As_4-flux in the MBE prior to growth, in order to remove the oxide layer from the substrate surface. The samples were grown at substrate temperatures between 480 °C and 620 °C. The As/Ga beam equivalent pressure ratio was close to 1.5 and the GaAs growth rate close to 1 $\mu m\ h^{-1}$. In these samples the background acceptor concentration was lower than 1×10^{14} cm^{-3} as determined from 'Polaron profiler' and CV measurements. In order to obtain a planar doping layer on a smooth surface, the growth of GaAs was interrupted by closing the Ga shutter and waiting for 10 s; then the Si furnace was opened either for 7.5 s or 30 s to deposit the doping layer of 2×10^{12} or 8×10^{12} atoms cm^{-2}, respectively. During the growth of GaAs the Si surface was kept at 1400 °C in order to obtain a Si flux as high as possible. The samples were grown with a buffer layer between the doping layer and the substrate of 2.5 μm and a top layer of 1 μm.

We first used the Van der Pauw method for the characterisation of the electrical transport properties of the samples. The subband population measurements

0268-1242/90/080861+06 $03.50 © 1990 IOP Publishing Ltd

were performed on Hall bar shaped samples. Ohmic contacts were made by annealing small Sn balls at 400 °C during 1.5 min under a N_2:H_2 = 4:1 flux. The Hall mobility and electron density were measured between 4.2 K and 300 K. The samples were illuminated with GaAs outgap radiation of a red LED ($\lambda = 650$ nm) mounted inside the cryostat.

We have grown two sets of samples with doping concentrations of 2×10^{12} cm^{-2} and 8×10^{12} cm^{-2} at three different substrate temperatures, 480 °C, 530 °C and 620 °C, see table 1. This table also shows the measured Hall density and mobility of the samples at 4.2 K. The results clearly show that the Hall mobility at 4.2 K increases by a factor of 2 when the growth temperature is decreased from 620 °C to 480 °C. The Hall electron density decreases when the growth temperature is lowered. After illumination the mobility in all samples increases, whereas the electron density stays almost equal. The observed mobility of 6760 cm^2 V^{-1}s^{-1} in sample A and 5150 cm^2 V^{-1}s^{-1} in sample D are the highest Hall mobilities in Si δ-doped GaAs samples at a sheet donor concentration of 2×10^{12} cm^{-2} and 8×10^{12} cm^{-2} reported thus far [7, 8].

Figure 1 shows the temperature dependence of the Hall electron density and mobility of the samples A, C, D and F between 4.2 K and 300 K before and after illumination. In the temperature range between 4.2 K and 100 K the Hall mobility in the samples A and D, grown at 480 °C, appears to be much higher than in the samples C and F, grown at 620 °C. In samples C and F, grown at 620 °C, the electron density below 100 K compares very well with the sheet doping concentration. On the other hand for samples A and D, grown at 480 °C, for both doping concentrations the electron density below 100 K appears to be smaller by almost a factor of 2. We note, however, that in δ-doped structures normally more than one subband is populated. These subbands have a different mobility. They thus add in a complicated way to the measured Hall voltage [9]. Hall measurements therefore in general give only limited information on the total electron density.

A method which is able to determine the electron density in the different subbands separately is based on the SdH effect. We carried out measurements on Hall-bar shaped samples in magnetic fields up to 20 T. The weak oscillations in ρ_{xx} and ρ_{xy} were resolved by measuring $d\rho_{xx}/dB$ and $d\rho_{xy}/dB$ with a modulation field of 0.03 T at a frequency of 70 Hz. The subband population has been determined by taking the fast Fourier transform (FFT) of $d\rho_{xx}/dB$ and $d\rho_{xy}/dB$. In sample D it was difficult to determine the exact population of the lowest subband due to the small number of weak oscillations visible in $d\rho_{xx}/dB$ and $d\rho_{xy}/dB$. The results for samples A and D are given in table 2. The total electron density, i.e. the sum of the electron densities in all the subbands, is smaller than the number of doping atoms deposited during growth for these samples. The total electron density in sample D is less than four times the total electron density in sample A although the doping concentration is four times higher. Illumination of sample A and D with a red LED only changed the subband population slightly.

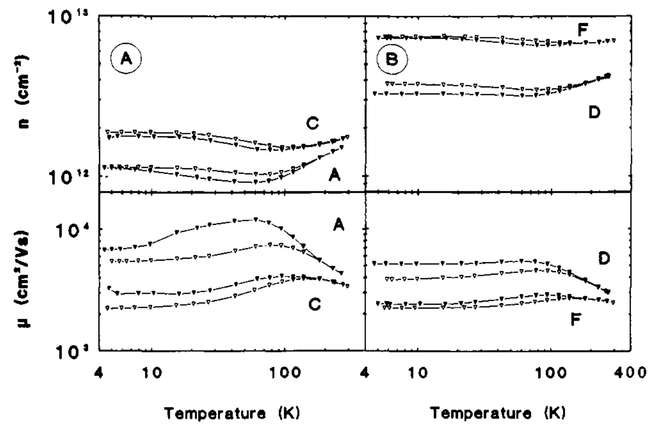

Figure 1. The measured temperature dependence of the Hall electron density and mobility between 4.2 and 300 K before illumination (open symbols) and after illumination (solid symbols) with a red LED in sample A, C, D and F, see table 1.

On the high-mobility samples A and D we also performed cyclotron resonance (CR) measurements. To our knowledge these are the first CR measurements on δ-doped samples reported thus far. The measurements were done in magnetic fields up to 20 T with an optically-pumped FIR laser. Figure 2 shows a typical example of a

Table 1. The sheet doping concentration, N_D, growth temperature, Hall electron density and Hall mobility at 4.2 K before and after illumination.

	N_D (cm^{-2})	T_{growth} (°C)	Electron density (cm^{-2}) dark	Electron density (cm^{-2}) light	Mobility (cm^2 V^{-1}s^{-1}) dark	Mobility (cm^2 V^{-1}s^{-1}) light
A	2×10^{12}	480	1.14×10^{12}	1.13×10^{12}	5450	6760
B	2×10^{12}	530	1.13×10^{12}	1.14×10^{12}	5170	6540
C	2×10^{12}	620	1.87×10^{12}	1.73×10^{12}	2230	3270
D	8×10^{12}	480	3.76×10^{12}	3.27×10^{12}	3850	5150
E	8×10^{12}	530	5.70×10^{12}	5.05×10^{12}	2260	2800
F	8×10^{12}	620	7.46×10^{12}	7.30×10^{12}	2240	2430

Table 2. The measured and calculated subband population n_i (10^{12} cm^{-2}) at 4.2 K in the samples A and D before and after illumination. The total electron density is given by n_{tot}. A square donor distribution of 20 Å and a background impurity concentration of 1 × 10^{14} cm^{-3} are used in the calculation.

		$d\rho_{xx}/dB$	$d\rho_{xy}/dB$	Calculated
A	n_0	1.37	1.37	1.38
	n_1	0.38	0.38	0.37
	n_{tot}	1.75	1.75	1.75
A_{ill}	n_0	1.50	1.53	—
	n_1	0.45	0.42	—
	n_{tot}	1.95	1.95	—
D	n_0	3.50	?	3.60
	n_1	1.23	1.24	1.29
	n_2	0.51	0.52	0.46
	n_{tot}	5.24	?	5.25
D_{ill}	n_0	3.50	?	—
	n_1	1.29	1.30	—
	n_2	0.56	0.55	—
	n_{tot}	5.35	?	—

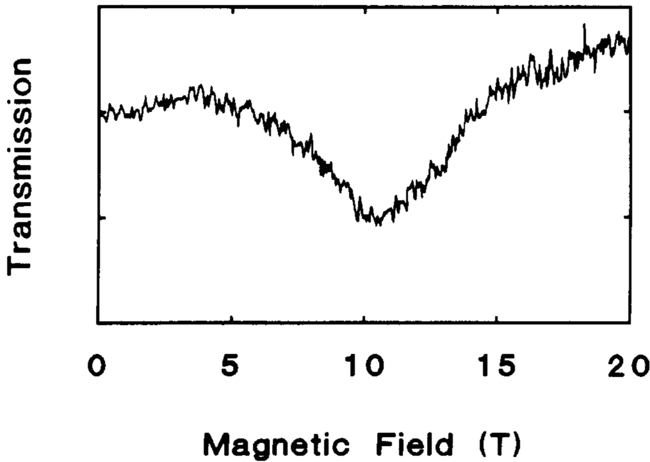

Figure 2. A measured FIR absorption profile as a function of the magnetic field at a wavelength of 77.4 μm at 1.3 K.

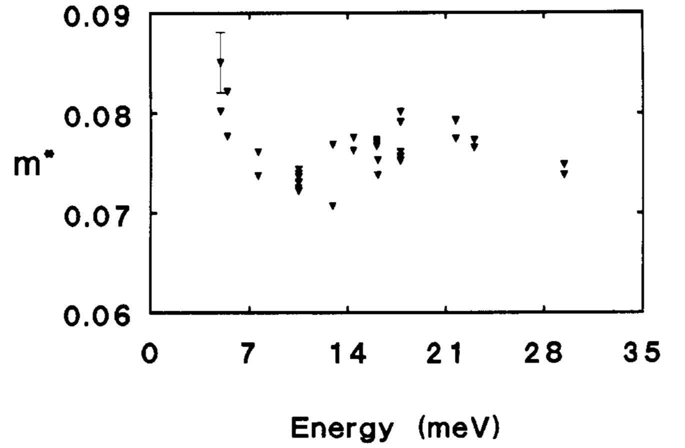

Figure 3. The effective mass determined from the magnetic field position of the minimum in the FIR absorption profile as a function of the energy of the CR at 1.3 K.

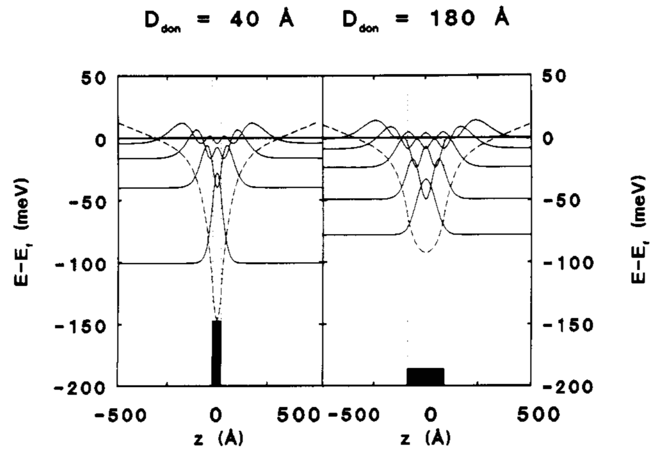

Figure 4. The calculated energy and probability distribution, $|\varphi_i(z)|^2$, of each subband (solid curves) and the electrostatic potential (broken curve) for a δ-doped structure. The 4.5 × 10^{12} cm^{-2} donors are distributed over 40 Å in (*a*) and over 180 Å in (*b*) as indicated by the black box.

measured CR profile. All measured CR profiles were very broad and some of them had an asymmetric shape. In figure 3 we have plotted the apparent cyclotron effective mass derived from the transmission minimum for sample D as a function of energy. Similar measurements on sample A showed a smaller value. The effective mass shows a complicated behaviour as a function of energy for both samples A and D.

3. Self-consistent calculation of the subband energies and envelope wavefunctions

We calculated the confining potential, subband energies and envelope wavefunctions self-consistently by solving simultaneously the Poisson and Schrödinger equations. Due to the high electron density in a δ-doped structure, more than one subband is populated. The distribution of the electrons over the subband was calculated taking into account the non-parabolicity of the Γ-conduction band [10]. In figure 4 we show as an example the probability distribution, $|\varphi_i(z)|^2$, and E_i in a δ-doped structure in which 4.5 × 10^{12} cm^{-2} donors are spread over 40 Å and 180 Å. It is clear from these figures that the distribution of the electrons over the levels is dependent on the width of the donor distribution. The width of the donor distribution can thus be used as a fitting parameter in the calculations to obtain the same sub-band population as measured.

We studied the influence of the exchange and correlation effects on the subband energies and envelope wavefunctions. Table 3 gives the calculated subband population and the energy of the lowest subband with and without the exchange interaction included, for samples with a width of the donor distribution of 100 Å (columns 1 and 2 of table 3). The calculations show that

Table 3. The relative population, n_i, of the subbands and energy of the lowest subband, E_0, calculated for:
(1) a square donor distribution of 100 Å with exchange interaction;
(2) a square donor distribution of 100 Å without exchange interaction;
(3) a Gaussian donor distribution of $25\sqrt{\pi}$ Å with exchange interaction.

		Relative subband population			Lowest subband E_0 (meV)		
N_{2DEG} (cm^{-2})	i	1	2	3	1	2	3
1.0×10^{12}	0	0.797	0.775	0.771	13.55	12.94	13.45
	1	0.203	0.225	0.229	—	—	—
4.5×10^{12}	0	0.594	0.583	0.581	25.60	25.16	27.43
	1	0.293	0.288	0.284	—	—	—
	2	0.100	0.105	0.110	—	—	—
	3	0.013	0.023	0.025	—	—	—
10.0×10^{12}	0	0.508	0.502	0.502	35.14	34.84	39.51
	1	0.304	0.299	0.293	—	—	—
	2	0.136	0.136	0.139	—	—	—
	3	0.049	0.053	0.054	—	—	—
	4	0.004	0.010	0.012	—	—	—

the influence of the exchange interaction on the subband population and energy is only weak.

We also studied the changes of the subband population and energies for the case of a Gaussian distribution of the donor atoms, $N_D(z) = 2/\sigma\sqrt{\pi}\exp(-z/\sigma)^2$, instead of a square distribution [1, 5, 11]. Calculations show that a Gaussian distribution with a half width $\sigma = (d/4)\sqrt{\pi}$ gives nearly the same subband population as a square distribution with a width d. This is shown in columns 1 and 3 in table 3 in the case of a square distribution with a width of 100 Å and a Gaussian distribution with a half width of $25\sqrt{\pi}$ Å. On the other hand, the subband energy is sensitive to the donor distribution if the electron density is high. We conclude that the shape of the donor distribution influences the calculated subband energy at high electron densities only.

4. Discussion

The subband population measured in samples A and D is in good agreement with the calculations for a square donor distribution donor with a width of 20 Å, see table 2. It is difficult to give a very accurate value for the width because below 20 Å the subband population is nearly independent of the width of the donor distribution. The total electron density found in sample A by the FFT on $d\rho_{xx}/dB$ and $d\rho_{xy}/dB$ is nearly equal to the intended donor concentration. Only a small fraction of the electrons is missing, probably due to the formation of a depletion layer on both sides of the δ-doped layer, see table 2. In sample D, however, the total electron density is much smaller than the sheet doping concentration. Zrenner *et al* [2] found that the electron density is not only dependent on the sheet doping concentration but also on the width of the donor distribution. They argued that this is due to the DX-centre at 200 meV above the Γ-band. For the same number of electrons originating from the same sheet doping concentration, subbands at higher energies are populated in samples with a narrower donor distribution. Thus a threshold of 200 meV is reached at a lower doping concentration than for a wider donor distribution. In this way the DX-centre levels off the maximum attainable electron concentration. In sample A the total electron density is such that the corresponding Fermi level lies well below 200 meV, whereas in sample D it does not.

If indeed DX-centres were responsible for the discrepancy of the electron density as described above, one should expect to observe the PPC effect. Suprisingly, however, the electron concentration has hardly changed after illumination of the sample. This means that there are no DX-centres at all and the arguments given above are wrong.

Recently Beall *et al* [12] presented SIMS and CV measurements on δ-doped GaAs structures in the same range of growth temperatures and doping concentrations. They found evidence that at doping concentrations above 4×10^{12} cm^{-2} only a fraction of the silicon is deposited on electrically active sides. The remainder of silicon forms clusters or at higher growth temperatures, above 590 °C, even small droplets. In view of their results we think that this mechanism is also responsible for the discrepancies between the electron concentration and the sheet doping concentrations found in our samples.

We have already discussed the discrepancy between the electron density derived from van der Pauw and SdH measurements. The Hall electron density in samples A and D is much smaller than the electron density derived from the FFT measurements. As stated before, this is due to the different mobilities in the different subbands. It is likely that the width of the donor distribution is larger in samples C and F, grown at high temperature, than in

samples A and D, grown at low temperatures. Table 4 shows that this is indeed true in the samples investigated. In this case for sample A and D a strong overlap between the envelope function and the scatterers exists only for the lowest subband, see figure 4. As a consequence we expect that the mobility in the various subbands differs more strongly in samples A and D than in samples C and F [13]. This is consistent with the observation that samples A and D show the strongest discrepancy between the van der Pauw and the SdH measurements.

Note that at room temperature the differences in electron densities determined from van der Pauw measurements for samples A and C are much smaller than at low temperature. This is not suprising, because at room temperature the scattering of electrons on optical phonons is the dominant scattering mechanism for all subbands involved. Thus the mobility in these subbands is not expected to differ that much.

When the subband population is known and only two subbands are populated we are able to calculate the subband mobility from the Hall electron density and mobility [9], see table 5. This proves that the mobility in the higher subbands increases when the distribution of the ionised donors becomes narrower. After illumination of sample A, the mobilities in the first and second subbands become 2150 $cm^2\ V^{-1}s^{-1}$ and 10 900 $cm^2\ V^{-1}s^{-1}$, respectively. We think that the mobility in the highest subband increases because the electron distribution is shifted away from the donors after illumination. This shift is due to the flat band conditions in the GaAs depletion layer which exist after neutralisation of the charged acceptors due to bandgap excitation. In sample D, where three subbands are populated, we can only estimate the mobility in the subbands. The mobility in the lowest subband at 4.2 K is $\approx 1500\ cm^2\ V^{-1}s^{-1}$ and in the other subbands $\approx 5500\ cm^2\ V^{-1}s^{-1}$.

Note that the mobilities observed in the narrow δ-doped conduction layers of samples A and D are much higher than the mobilities reported thus far [5, 7]. In addition to the mechanism described above, there may be a second mechanism which enhances the mobility. As van Hall *et al* [14] have shown, in a heterostructure the electron scattering is determined by the fluctuations in the distribution of the ionised scattering centres. It is likely that in samples grown at low temperature, like samples A and D, these fluctuations are smaller than in samples grown at high temperature, like samples C and F.

We now turn to measurements of the CR. As mentioned already, the widths of the CR are very broad compared with the width of the CR in a $GaAs/Al_xGa_{1-x}As$ heterostructure. There are at least three reasons for this broadening. First, the mobility and hence the scattering time of the electrons in the δ-doped layer is low compared with the case of a heterostructure. Second, the high electron density gives rise to considerable dielectric broadening of the CR (see [15] and especially figure 4 therein). Third, the overlap of several CRs may also give rise to an apparent broadening of the CR profile. Remember that more than one subband is populated.

In the case that the minimum in the FIR absorption is due to a CR in only one subband we can determine the effective mass of the electrons. We find that the effective mass in sample D is considerably enhanced above the effective mass at the Γ conduction band minimum. Since the electron density is very high in these structures and the confining potential is very narrow it is likely that this enhancement is due to the non-parabolicity of the Γ conduction band. The effective mass which we obtained is, however, lower than that expected from the calculations of Rössler [10]. In sample A the effective mass is smaller than in sample D and very close to the effective mass determined in bulk GaAs. This is also consistent within the picture of non-parabolicity because the electron density in sample A is much smaller than in sample B. At present we cannot explain the complicated behaviour of the effective mass as a function of the CR energy.

Table 4. The width of the donor distribution in all samples as determined from the SdH measurements.

	T_{growth}		
n_{don} (cm^{-2})	480 °C	530 °C	620 °C
2×10^{12}	20 Å	30 Å	60 Å
8×10^{12}	20 Å	80 Å	?

Table 5. The mobility in the two subbands of the samples A, B and C each with a sheet doping concentration of $2 \times 10^{12}\ cm^{-2}$.

	A	B	C
μ_0	2210	2030	2230
μ_1	9250	8500	2230

5. Conclusion

In conclusion, we have shown that for the growth of narrow silicon δ-doped layers in GaAs a lower substrate temperature is fortuitous. Measurements on the subband population using the SdH effect show that the δ-doped samples we have grown at 480 °C display very narrow doping profiles, down to 20 Å. In these very narrow δ-doped layers the mobility is enhanced strongly. To our knowledge these samples show the highest mobility reported to date. We think that the enhancement of the mobility is due to a smaller overlap of the ionised donors with the electrons in the higher subbands. In these very narrow δ-doped layers we were able to determine the effective mass by CR measurements for the first time. The results show that in a sample with a high electron density the effective mass is considerably enhanced.

References

[1] Zrenner A, Reisinger H, Koch F and Ploog K 1985 *Proc. 17th Int. Conf. Physics of Semiconductors (San Francisco 1984)* ed J P Chadi and W A Harrison (Berlin: Springer) p 325

[2] Zrenner A, Koch F, Williams R L, Stradling R A, Ploog K and Weimann G 1988 *Semicond. Sci. Technol.* **3** 1203

[3] Zeindl H P, Wegehaupt T, Eisele I, Oppolzer H, Reisinger H, Tempel G and Koch F 1987 *Appl. Phys. Lett.* **50** 1164

[4] Wenchao Cheng, Zrenner A, Qiu-Yi Ye, Koch F, Grützmacher D and Balk P 1989 *Semicond. Sci. Technol.* **4** 16

[5] Beall R B, Clegg J B and Harris J J 1988 *Semicond. Sci. Technol.* **3** 612

[6] Santos M, Sajoto T, Zrenner A and Shayegan M 1988 *Appl. Phys. Lett.* **53** 2504

[7] Gillman G, Vinter B, Barbier E and Tardella A 1988 *Appl. Phys. Lett.* **52** 972

[8] Ploog K 1987 *J. Cryst. Growth* **81** 304

[9] Smith R A 1978 *Semiconductors* (Cambridge: Cambridge University Press)

[10] Rössler U 1984 *Solid State Commun.* **49** 943

[11] Ullrich B, Schubert E F, Stark J B and Cunningham J E 1988 *Appl. Phys.* A **47** 123

[12] Beall R B, Clegg J B, Castagné J, Harris J J, Murray R and Newman R C 1989 *Semicond. Sci. Technol.* **4** 1171

[13] Schubert E F, Cunningham J E and Tsang W T 1988 *Solid State Commun.* **63** 591

[14] van Hall P J, Klaver T and Wolter J H 1988 *Semicond. Sci. Technol.* **3** 123

[15] Singleton C J G M, van der Wel P J, Perenboom J A A J, Barnes D J, Hopkins M A, Nicholas R J and Foxon C T B 1988 *Phys. Rev.* B **38** 13133